Proceedings of the ASME Symposium on Elevated Temperature Application of Materials for Fossil, Nuclear, and Petrochemical Industries
March 25-27, 2014

A COMBINED EXPERIMENTAL-COMPUTATIONAL APPROACH TO DESIGN OPTIMIZATION OF HIGH TEMPERATURE ALLOYS

Rajesh Jha
Florida International University, MAIDROC Lab.
Miami, Florida, U.S.A.

George S. Dulikravich
Florida International University, MAIDROC Lab.
Miami, Florida, U.S.A.

Frank Pettersson
Åbo Akademi University
Åbo, Finland

Henrik Saxén
Åbo Akademi University
Åbo, Finland

Nirupam Chakraborti
Indian Institute of Technology
Kharagpur, West Bengal, India

ABSTRACT

Experimental data were used to develop metamodels to predict high temperature alloy chemistry trends influencing stress-to-rupture and time-to-rupture of Nickel based superalloys. Chemistry optimization utilized evolutionary neural networks, bi-objective genetic programming and pruning algorithm. Optimization results were compared with the experimental data and IOSO optimization algorithm. Response surfaces were developed through various modules available in a commercial optimization package. Pareto optimized chemistries were tested using thermodynamic database, FactSage^{TM}, by studying the phase distribution as a function of temperature of manufacture and exposure. Uniformity in the amount of critical phases over 0-1200 ^{0}C range confirmed high temperature stability for optimized alloys.

INTRODUCTION

Multi-component superalloys, because of their superior high temperature and corrosion resistant properties, are extensively used in many specialized high-tech applications in aeronautical, nuclear and petrochemical industry [1-4]. Superalloys are most often used for high temperature applications which are in excess of 70 percent of the absolute melting temperature. Hence, such alloys must be resistant to oxidation and hot corrosion. Additionally, they must resist mechanical forces such as creep, fatigue and thermo mechanical fatigue. Superalloys can be based on Iron, Cobalt, Titanium, Nickel, *etc*. Nickel based alloys and Ti based alloys are best suited for high temperature applications [5] (Figure 1). At the same time, further retention of high performance properties at extremely high temperatures implies use of expensive rare earth elements.

Modern Ni-based superalloys usually contain more than ten alloying elements along with some impurities. The various alloying elements enhance different properties of the alloys as follows.

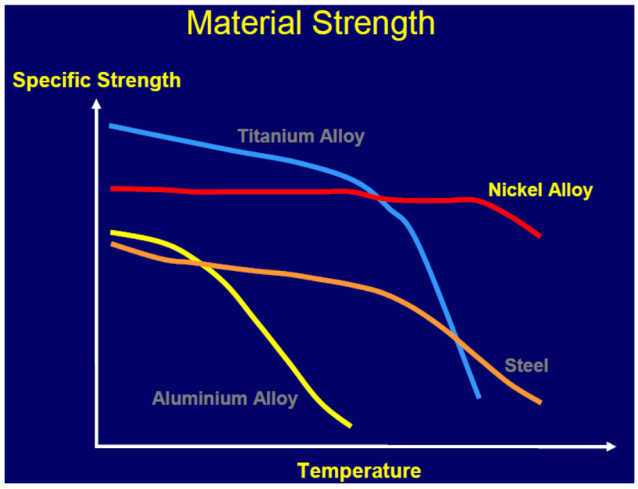

Figure 1: Relative comparison of various alloy systems [5].

1. Cobalt, Chromium, Iron, Molybdenum, Tungsten, Tantalum, Rhenium basically enhance solid solution strengthening.
2. Chromium, Titanium, Niobium, Hafnium, Molybdenum, Tungsten, Tantalum enhance grain boundary strengthening with carbides.
3. Aluminium and Titanium generate a two-phase equilibrium microstructure with Nickel, gamma (γ) and gamma-prime (γ') which enhances the elevated-temperature strength of the alloy and is also responsible for resistance to creep deformation.
4. Aluminium, Chromium, Yttrium, Cerium and Lanthanum improve the oxidation resistance,
5. Chromium, Cobalt, Silicon, Thorium and Lanthanum improve hot corrosion resistance,
6. Boron, Carbon, Zirconium and Hafnium act as grain boundary strengthening (refining) agents.

The concentration of various alloying elements is very important in determining the microstructure of an alloy and consequently multiple macroscopic properties of the alloy. Even

a slight deviation in the concentration may affect the composition of a phase responsible for the desired property.

The correlations among the multiple alloying elements and between the alloying elements and the desired alloy properties are quite complex to determine statistically. It may cost a fortune to determine them experimentally, mainly because of a need for very large experimental data sets [6, 7] when using artificial neural networks as interpolants and due to inadequate information and limited available database for the associated multi-component phases and their associated equilibria.

Purely computational approach based on *ab initio* methods and non-equilibrium thermodynamics of solids has a major drawback of exorbitant computing time required to predict properties of any alloys having more than three alloying elements.

Reality is such that high performance steel alloys need a large number of alloying elements in order to create a large enough function space for multiple often contradicting objectives (multiple properties of alloys) to be extremized simultaneously [8-22]. Thus, in order to develop a new family of alloys or enhance the properties of an existing alloy in an affordable and verifiable manner, one has to combine experimental data and sophisticated multi-objective evolutionary optimization algorithms [8-10] utilizing accurate response surfaces [23-27] or genetic programming [28-32] as a metamodel or a combination of molecular dynamics [33, 34], thermodynamics [18, 35] and artificial neural networks [36-40] in order to develop the best tradeoff (Pareto optimum) superalloys.

The current work is inspired by an earlier work [12-15], where an evolutionary search multi-objective optimization algorithm [44] combined with artificial neural networks and self organizing response surface method was used [26] together with experimental verification to develop chemical concentrations for a realistic family of optimized Ni based superalloys containing 12 alloying elements [15].

In the present work, we made an attempt to further strengthen the evolutionary approach applied to design of the alloy composition for Ni based super alloys for desired objectives, by further exploring a number of emerging evolutionary paradigms and supporting our findings by thermodynamic calculations. Further, a commercial optimization package was used [45], where a number of response surface generation methods were exercised. The subsequent use of a multi-objective optimizer on such hyper-surfaces to search for the optimized multiple alloy properties was followed by thermodynamic calculations [46].

It should be pointed out that this general combined experimental-computational design optimization method is applicable to arbitrary alloys [11, 13, 18, 19, 20].

It should also be pointed out that it is a common knowledge that thermal and/or mechanical after-treatment of alloys are equally important in determining their macroscopic properties [20]. In this work, we did not include simultaneous optimization of thermal treatment protocols for superalloys.

THE SUPERALLOY SYSTEM

Concentrations of each of the alloying elements in the initial batch of 120 Ni based superalloys were generated using Sobol's quasi-random sequence generation algorithm [44]. These alloys were then manufactured and their mechanical properties evaluated using standard experimental procedures [15]. The chemical elements that were considered to be important were identified as Ni, C, Cr, Co, W, Mo, Al, Ti, B, Nb, Ce, Zr, Y, while elements such as S, P, Fe, Mn, Si, Pb, Bi were treated as extraneous impurities. Out of the twelve significant alloying elements, a total of seven appeared to be the major property changers and were chosen for developing response surfaces and further for optimization. Thus, the chosen elements whose concentrations were optimized were Ni, C, Cr, Co, W, Mo, Al, Ti . Their compositional bounds are presented in Table 1 in Annex. Concentrations of Nb, B, Ce, Zr, Y in all sample alloys were kept constant at 1.1%, 0.025%, 0.015%, 0.04%, and 0.01%. All 120 initial alloys were tested for their *stress-to-rupture* (N/mm^2) and the *time-to-rupture* (hours) [15]. It should be noted at this point that owing to some experimental limitations, the stress-to-rupture was measured at the room temperature, while the time-to-rupture was measured for a constant stress of 230 N/mm^2 at a temperature of 975 ^{0}C.

Multi-objective optimization problem was formulated as: Simultaneously maximize stress-to-rupture at room temperature and time-to-rupture at 975 ºC at a fixed stress of 230 N/mm^2.

Since higher stress would lead to a quicker rupture, the objectives are mutually conflicting, and lead to a Pareto-optimal solution [9, 10], that is, the best trade-off solutions.

From Table 1, it can be noted that the upper and lower bounds of the design variables (concentrations of alloying elements) are different and the variation is quite large. For example, among the design variables, bounds on Mo are about 10 times that of C. At the same time, bounds on Co, Cr and W are further 5 – 10 times that of Mo. On the objective front, bounds of time-to-rupture are 2-10 times that of Co, Cr and W, while, bounds of stress-to-rupture are 10 times that of time-to-rupture. Hence, the range of values varies widely, that is, the bound for stress-to-rupture is about 5,000-10,000 times that of Carbon (C) concentration while others are in between.

Working with this dataset may lead to improper functioning in some machine learning algorithms, [45]. Hence, it is recommended to normalize the dataset for proper functioning of various approaches for development of response surface, [45, 46]. In this work, the dataset was scaled between 0 and 1.

METAMODELING AND RESPONSE SURFACES

Meta-models were constructed for both *stress-to-rupture* (σ_R) and *time-to-rupture* (τ_R) for these alloy systems using the compositional and experimental data of the 120 initial alloy samples discussed above. Three different methodologies were used for this purpose: (i) Evolutionary Neural Net (EvoNN) [29-30, 32, 34, 36-39], (ii) Bi-objective Genetic Programming (BioGP) [28-31] and a (iii) Pruning Algorithm (PA) [40]. The reader can consult the cited references for information on salient features of each of these approaches. In adapting these models,

the square sum of errors between the observed and predicted quantities was used as the main objective expressing the quality of the fit of the experimental data. Pruning Algorithm (PA) [40] was used for modeling to supplement and corroborate the information generated by EvoNN and BioGP. Subsequent analysis of this model set is helpful in identifying the most important or relative importance of inputs and connections for an efficient model construction as can be seen in Figures 2 and 3. In these fifures, a large number of models of stress-to-rupture have used Mo as an essential input followed by W, Al, Ti and Cr. For the time-to-rupture models, Cr was used predominantly, followed by Ti, Co and C. The role played by these essential elements is reasonably well understood from the basic physical metallurgy of the Ni-based superalloy systems [1-5].

Among the predominant elements, Mo is known to contribute towards solid solution strengthening of the γ phase due to its significantly different electronic structure and atomic radius compared to Ni. Tungsten is also known to have similar effect and as a result, the stress-to-rupture increases. The Al and Ti contribute towards the formation of the γ' phase. Though both γ and γ' belong to a cubic lattice, the small mismatch between them is however enough to impair dislocation movements, leading to improvements in both stress and time-to-rupture. It is also well known that Cr initially forms the primary carbide CrC during solidification, which during heat treatment dissociates into other carbides. This Cr depletion leads to further γ' precipitation at the carbide interface, leading to additional strengthening. It needs to be emphasized, once again, that the pruning models [40] could quite efficiently identify these essential inputs from the experimental data as shown in Figures 2 and 3.

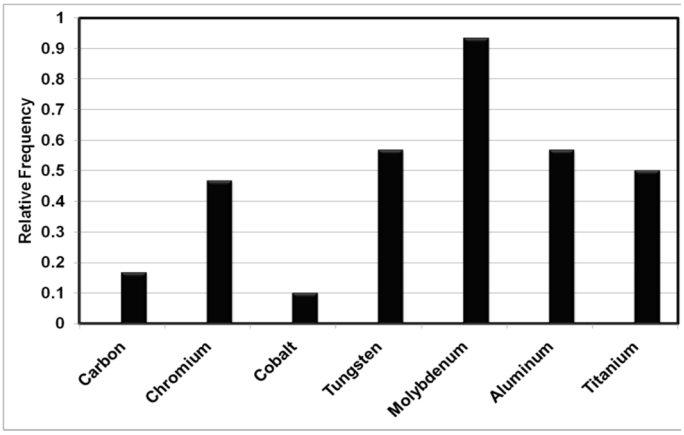

Figure 2: Relative frequency of design variables affecting stress-to-rupture

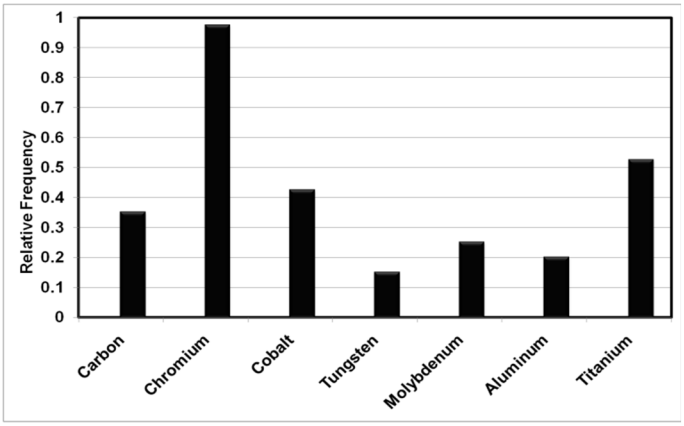

Figure 3: Relative frequency of design variables affecting time-to-rupture

Additionally, response surfaces were developed by various modules available in a commercial optimization software package, modeFRONTIER [42], *e.g.,* Radial Basis Function (RBF), Kriging (KR), Anisotropic Kriging (AKR), Gaussian Processes (GP), Polynomial Singular Value Decomposition (SVD) and Evolutionary Designs (ED). The various methods for generation of multi-dimensional response surfaces, that is, RBF, KR, AKR, GP, SVD and ED, were tested on the same experimental data set from which it was created. Scatter plots were created between experimental data and the predicted output and it was linearly fitted in order to estimate accuracy of the model. The deviation from the 45 degree line (that is, linearly fitted experimental *vs*. actual experimental plot) represents the error associated with the particular model and it was tabulated as the correlation coefficient values as shown in Figure 4, Figure 5 and Table 2 in the Annex.

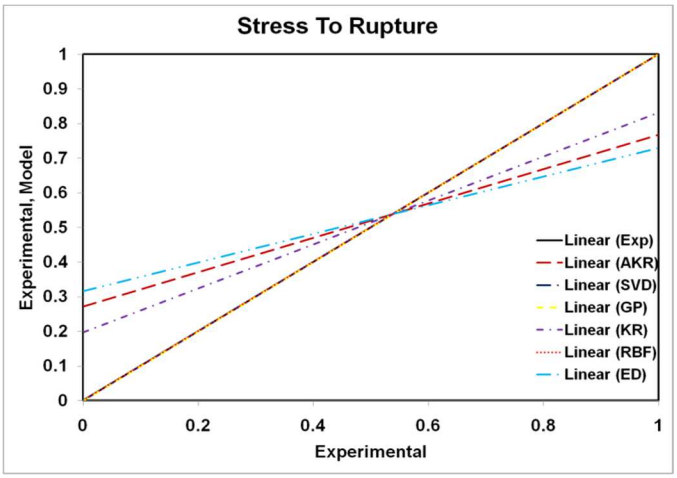

Figure 4: Linear fit for estimation of accuracy of the model for stress-to-rupture

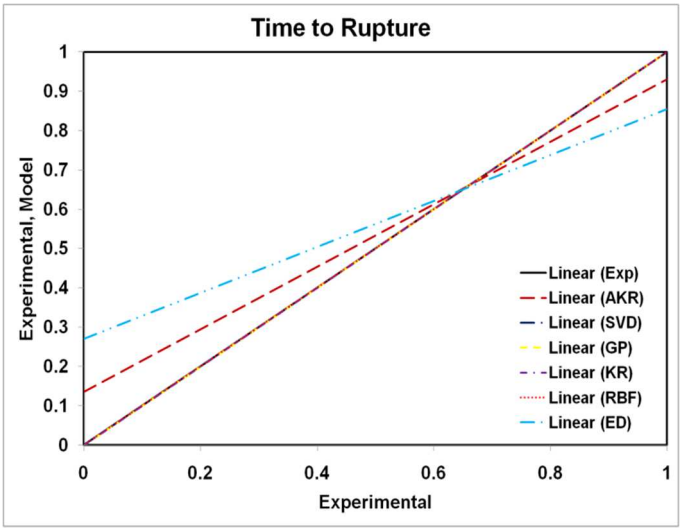

Figure 5: Linear fit for estimation of accuracy of the model for time-to-rupture

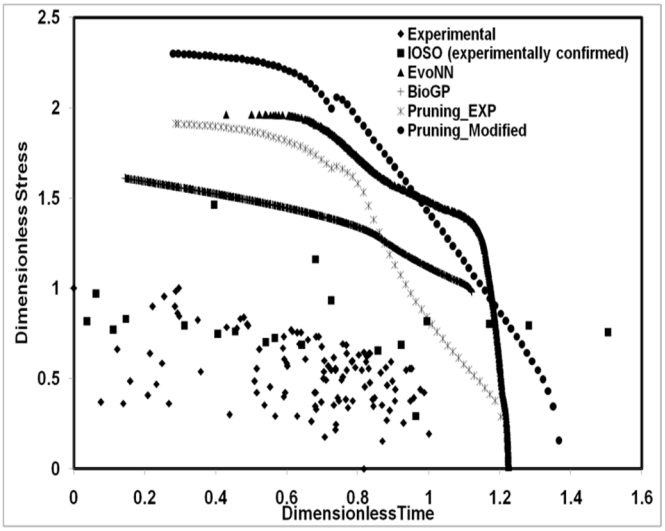

Figure 6: Comparison among the Pareto optimal alloys obtained through various approaches

MULTI-OBJECTIVE OPTIMIZATION

For the metamodels obtained through EvoNN, BioGP and the pruning algorithm, the multi-objective optimization problem formulated above was solved by using a real coded predator-prey genetic algorithm described elsewhere [36] for the EvoNN and BioGP model, while Sequential Quadratic Programming (SQP) algorithm [29, 47] was used for the pruning algorithm. During the optimization, the design variables, which are the concentrations of the alloying elements, were kept within the bounds mentioned in Table 1, while there was no such bound on the objectives which were allowed to explore the search space.

Initially, the optimization with the pruning algorithm models for stress-to rupture and time-to-rupture were conducted within the bounds in the variable space shown in Table 1. Later on, to see if any better solutions exist beyond these boundaries, the upper bounds were increased by 5 % and the lower bounds were lowered by 5% and the optimization was conducted once again to look for any potential differences.

Attempts were also made to carry out this optimization task using a stochastic approach known as Indirect Optimization based upon Self-Organization algorithm (IOSO) [8, 11-19, 41] which is based upon a novel response surface strategy. It uses a self-adapting response surface formulation, where the first stage involves creating approximations of the objective functions.

The comparison between the experimental data, experimentally confirmed data predicted by IOSO methodology and the data predicted by EvoNN, BioGP and pruning algorithm are shown in the Figure 6. For the models developed by various response surface modules available in modeFRONTIER software [42], that is, RBF, KR, AKR, GP, SVD and ED, a number of optimization techniques were used to solve the multi-objective problem formulation discussed before.

The models developed through various methodologies mentioned above, were used to solve the multi-objective optimization problem formulated before in the text.

Optimizers (available in modeFRONTIER [43]) used for this purpose are enlisted below:

a) Non-dominated Sorting Genetic Algorithm II (NSGA2) [10]: The following variants of NSGA2 available are enlisted below:
   I. Original NSGA2
   II. Controlled Elitism
   III. Variable Population size
   IV. Steady State Evolution

b) Multi-Objective Particle Swarm Optimization (MOPSO)

c) Multi Objective Simulated Annealing (MOSA)

d) This fast optimizer uses response surface models (metamodels) to speed up the optimization process (FAST). The search algorithms used here are:
   I. NSGA2
   II. MOSA
   III. MOPSO
   IV. Multi-objective Genetic Algorithm (MOGA2)

e) HYBRID: an algorithm combining the global exploration capabilities of genetic algorithms along with the accurate local exploitation guaranteed by SQP implementations.

The results obtained by each of these optimization techniques were further ranked and the best available solutions from each RSM module were reported. A comparison among the solutions from various modules of modeFRONTIER along with the experimentally confirmed IOSO results can be seen in the Figure 7.

In this paper, the optimization was performed so that the upper and lower bounds of the design variables were maintained within the bounds of the experimental data [15]. While for the objectives, the upper bound was relaxed by 10 % in order to

explore the search space for superior solutions by using different response surface generation algorithms, while maintaining the chemical composition same as that reported from the experimental data [15]. The basic purpose was to search for superior solutions for the same alloy composition.

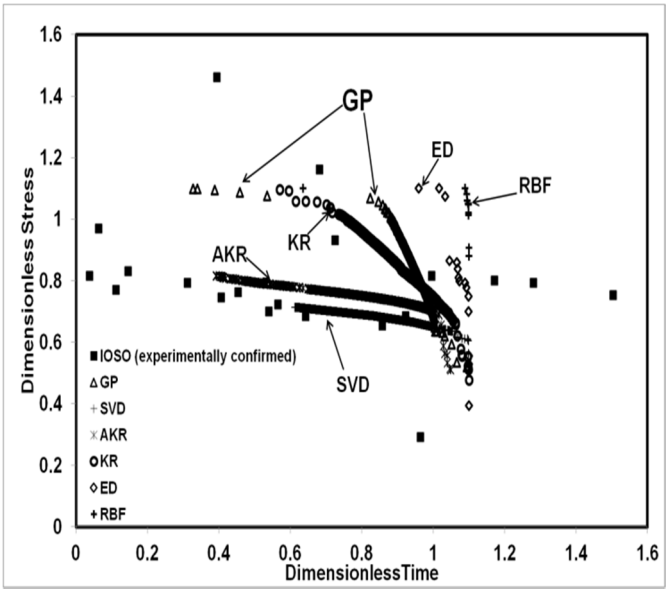

Figure 7: Comparison among the Pareto optimized alloys obtained using various response surface modules in modeFRONTIER [42] against those obtained via IOSO [13]

THERMODYNAMIC CALCULATIONS

The various properties of the superalloys can be directly attributed to various phases that form during their synthesis and application condition. The thermodynamics and kinetics of the formation and stability of a certain phase are beyond the scope of data driven model. From the optimization and comparison, one can easily infer that it is certainly possible to enhance a certain desired property while maintaining the design variables within the specified bounds, but in order to better understand the reason for this improvement, one needs to understand the phase equilibria in these alloys for synthesis and application point of view. In this work, this problem was attempted by using a thermodynamic database, FactSage™ [43].

Pareto optimized candidate whose properties were close to the experimentally confirmed solutions predicted by IOSO were chosen for thermodynamic validation. In this work, phase equilibria of one solution per each response surface generation method is presented. The phase equilibria studied through FactSage™ software provided detailed information about the phase distribution in all the selected alloys and has been tabulated in Table 3. Table 4 and 5 present the major constituents present in the alloys selected from the various methodologies at temperatures 25^{0}C and 975^{0}C, that is, the temperature at which the stress-to-rupture test was performed and the temperature at which time-to-rupture test was performed. In the Figures 8 (a-f), phase equilibria for the temperature range from 25^{0}C – 1200^{0}C is reported as the alloy was synthesized by heating up to 1200^{0}C and then cooling it to the room temperature, which here was assumed to be at 25^{0}C.

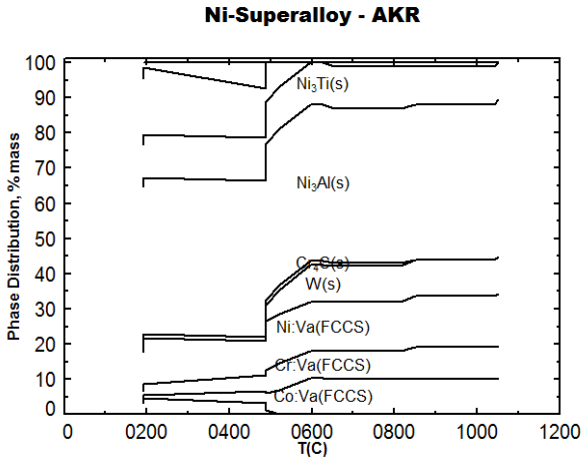

8:(a)

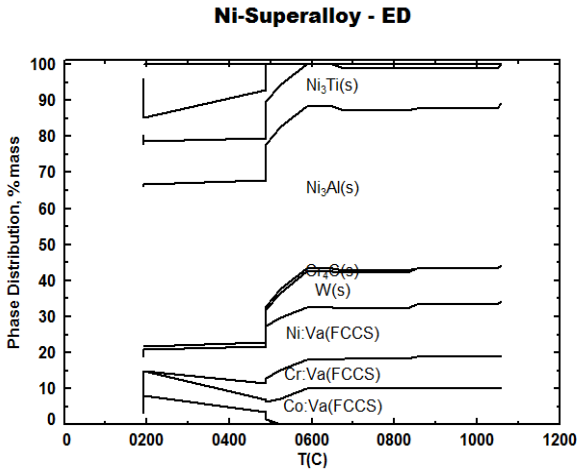

8:(b)

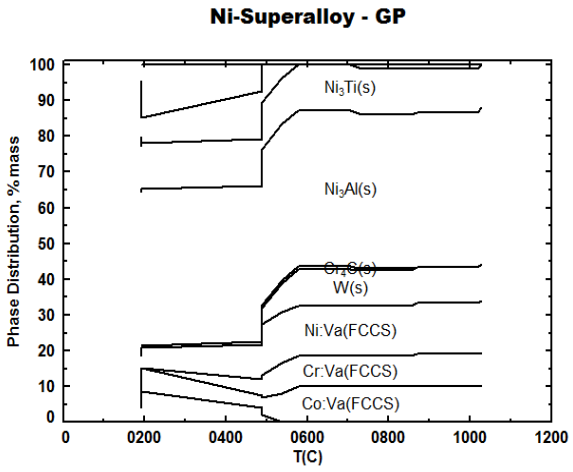

8:(c)

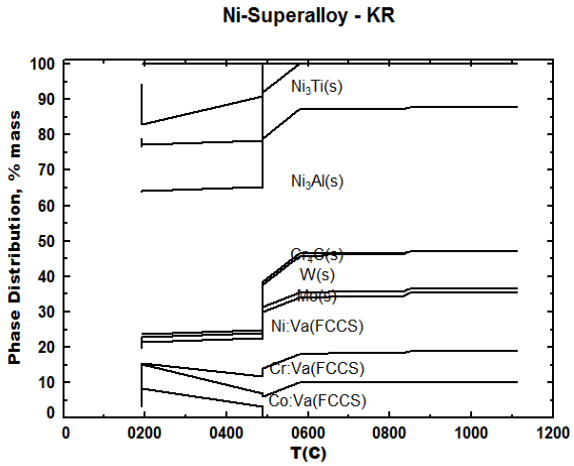

8:(d)

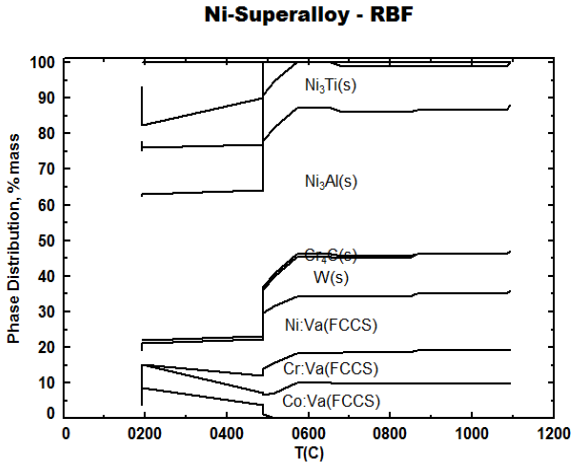

8:(e)

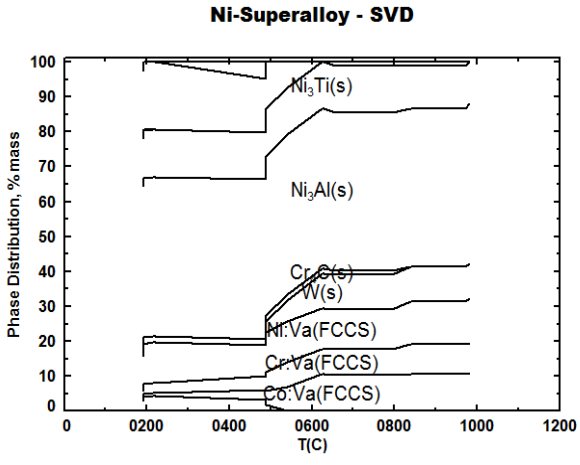

8:(f)

Figure 8: (a – f) Phase distributions *vs.* temperature for selected Pareto-optimized alloy candidates obtained using different response surface generation modules [42]

RESULTS AND DISCUSSION

Response Surface Generation

The response surfaces generated by various methodologies, *e.g.,* EvoNN, BioGP and pruning algorithm were associated with certain degree of error, but at the same time, they provided useful insight to the alloy system. Particularly, results obtained by pruning algorithm helped in determining the relative effect of the design variables on the properties which is well understood from the literature available for these alloy system.

Response surfaces were also generated by various modules available in modeFRONTIER [42]. A few modules, *e.g.,* SVD, GP and RBF were quite accurate as can be seen from the correlation values of linear fit of the data predicted by it for the input data from which it was created. This must be further tested for the data outside the prescribed bounds of design variables and this task can be included in the future work. Other response surface generation modules such as AKR, KR and ED had significant amount of error, of which ED was the worst (Figure 4 and Figure 5). This could be attributed to improper choice of functions and it will be included in the future work.

Multi-objective Optimization

For EvoNN, BioGP and pruning algorithms, it can be seen (Fig. 6) that the optimized alloys have superior properties compared to the initial 120 alloys. A few of the optimized alloys were also superior to the experimentally confirmed values predicted by IOSO (Fig. 6) [15]. Some of the resulting optimized alloys were close to the IOSO results, hence pointing to the fact that these results are achievable since all alloys designed by IOSO were experimentally verified [15].

In modeFRONTIER [42], the optimized results were in close vicinity with the experimentally confirmed IOSO predictions and a few even dominated it. Hence, it can be inferred that the predicted alloys are achievable. Another aspect of this predicted output is that the Pareto fronts obtained by various methodologies did not converge. This can be attributed to the fact that each of these search algorithms implemented different search techniques, and hence there is a possibility that due to this the search algorithms explored different parts of the search space and terminated in local optima. Apart from ED and RBF predictions, all other approaches had a well defined Pareto frontier. However, ED and RBF predictions were found to be concentrated in a small region and the improvement of it can be added to the future work. As it has been pointed out earlier in the text, the objectives were relaxed by 10 %. Hence, the result from modeFRONTIER was not compared to EvoNN, BioGP and Pruning Algorithm, as in these there was no bound on the objectives and these solutions will dominate the result of modeFRONTIER predictions.

Thermodynamic Validation

In order to proceed further towards synthesis of these optimized alloys for the desired or rather enhanced properties,

one must look into the thermodynamic feasibility and phase equilibria [43] of the constituent phases as a function of temperature of synthesis and application.

In short, the findings can be summarized as:

1. Nickel rich matrix (FCC) (γ phase) is ductile at all temperatures. It possesses moderate strength which decreases with temperature. In this study, it can be seen that there is considerably smaller amount of FCC-Nickel in elemental form in the results optimized through various methodologies.
2. It can be seen that the amount of Ni_3Al or γ' phase is present in large amounts and also its amount does not change in the optimized alloys with the temperature. γ' phase is brittle except at high temperatures. It possesses very high strength which increases with temperature up to about 830 °C.

The presence of γ' phase which is responsible for the strength of Ni-based superalloys is insensitive to temperature. In the present study, calculations suggest that the amount of these phases was constant at these temperatures. Hence, these alloys can be used for high temperature applications from thermodynamic point of view.

A close examination of Table 4 reveals the presence of a very high level of Ni_3Al (s) phase and Ni_3Ti (s) in all the optimized alloys. Together, these two phases constitute well over 50 wt% which is quite significant and it explains the superior properties of these optimized alloys. It is well-known [1-3] that in Ni-based superalloys, both Ni_3Al (s) and Ni_3Ti (s) constitute the γ' phase that forms in the FCC Ni (γ) matrix and leads to the superior strengthening of these alloys. Thermodynamic calculations confirm that this is happening in the optimized alloys, and the strengthening is further aided by the presence of the remaining alloying elements. The obtained results are thus meaningfully corroborated by the existing theory. Additionally, uniformity in the amount of major critical phases, *e.g.,* Ni_3Al (s) and Ni_3Ti (s), over temperature range (0-1200 °C) confirmed high temperature stability for alloys with maximized stress-to-rupture and time-to-rupture.

In summary, this study successfully demonstrated the efficacy of response surface methodology in determining the complex interrelationship between various design variables and desired macroscopic properties of alloys. It also demonstrated the advantage of implementing evolutionary data driven modeling and optimization in designing Ni based superalloys. Thermodynamic validation ensures that the work is proceeding in the right direction and can be implemented.

HIGH TEMPERATURE MAGNETIC ALLOYS (Al-Ni-Co)

AlNiCo magnets [48] are permanent magnetic alloys based on the Al-Ni-Fe-Co system. Magnetic property is mainly attributed to the presence of BCC iron and cobalt and it decreases with increasing temperature. In addition to limited literature available on these systems, one of the major challenges in designing such an alloy is maintaining the BCC phase during synthesis and to ensure that this phase will be retained at working or elevated temperatures. Meta-modeling combined with thermodynamic validation can prove to be a good alternative to avoid a large number of experiments otherwise needed in designing these alloy systems.

In our present work, Sobol's algorithm [44] was used to randomly generate alloy composition for the systems for which data is available in the literature while maintaining the prescribed bounds. The distribution of concentrations between a few of these can be seen in Figure 9.

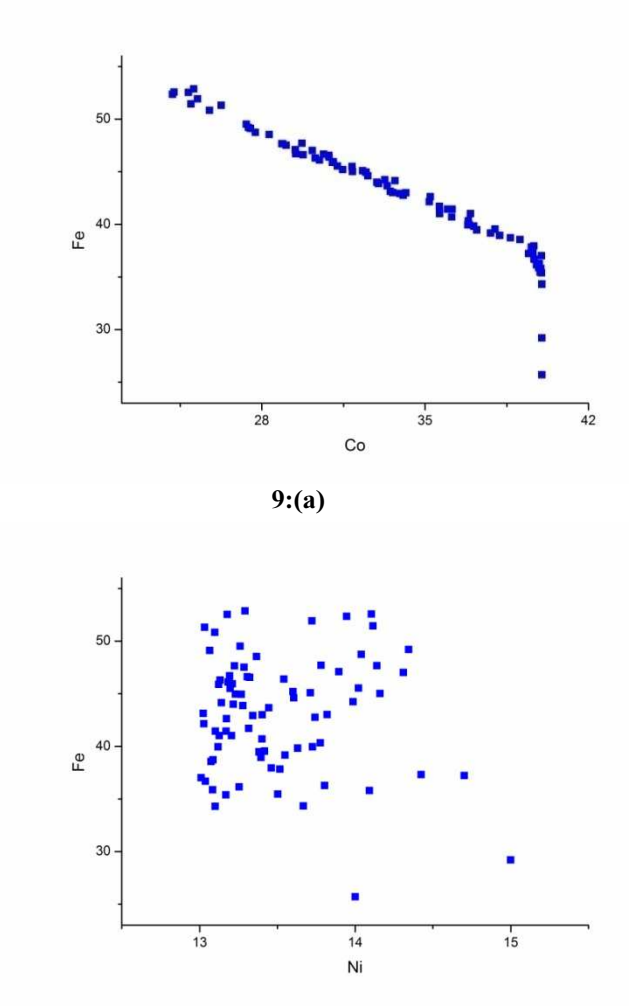

Figure 9 (a) – (b) : Distribution of concentration of alloying elements for a given AlNiCo family of alloys generated using Sobol's algorithm [44].

Thermodynamic validation of this AlNiCo alloy system was performed using FactSage [43] in order to determine the magnetic property and stability of the phases responsible for the magnetic property as well as the effect of temperature variation on this system. A few plots will demonstrate the variation of these phases with the temperature in Figure 10.

From these figures it can be seen that the BCC transforms to FCC and this transformation initiates at a lower temperature and increases with the temperature. At about 820 ºC, almost all of the

BCC is transformed to FCC and hence the AlNiCo material loses its magnetic property.

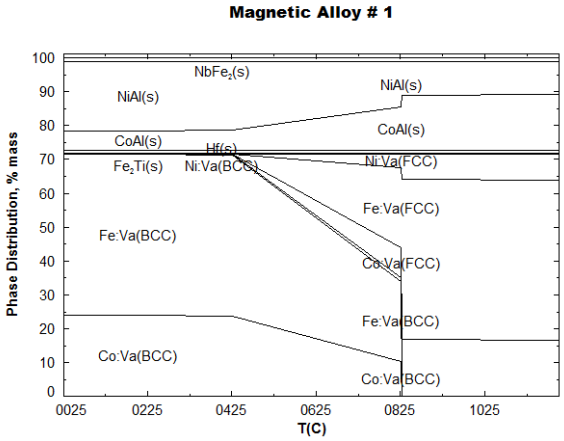

10:(a)

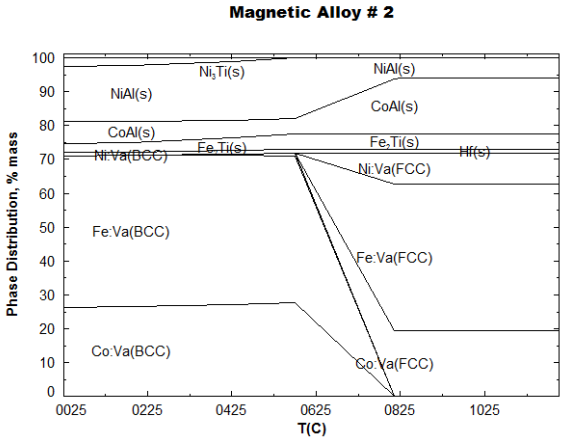

10:(b)

Figure 10(a)-(b): Phase distribution and variation with temperature for two of the generated AlNiCo alloys.

These calculations and the graphical representation can prove to be an asset prior to preparation for experimentation and optimization and can provide critical information regarding the transformations that need to be avoided in order to achieve the desired high temperature properties. All the candidate alloys were nonmagnetic with Curie temperature around the room temperature for the BCC and the Neel's temperature around -190 °C to -200 °C for the FCC. Hence, this confirms that all the alloys are non-magnetic at the synthesis temperature and also at the operating conditions. This information can be well utilized while designing the hard magnetic Al-Ni-Co alloys as it must retain they magnetic property at elevated temperatures, though some of the constituents are the ones that are present in non-magnetic Ni-based superalloys studied at present.

FUTURE WORK

In order to proceed further towards synthesis of these alloys, an attempt is to be made regarding a few differences in our calculations and predictions from various modules.
The future research tasks can be listed as:

1) Improve the accuracy of the developed response surface generation methods, ED in particular, and check their efficacy outside the prescribed bounds.
2) In the optimization part, attempts are to be made in order to converge to the same Pareto frontier obtained from various optimization methodologies.
3) In thermodynamic validation, attempts must be made to search for databases that may be beneficial in estimating the desired macroscopic properties of alloys in addition to the discovered phases.
4) Implement an in-house developed version of response surface methodology and multi-objective hybrid optimizer, in order to explore the search space for further improvements [25-26, 49-57].
5) Apply this alloy design methodology in designing the hard magnetic Al-Ni-Co- alloys for high temperature applications.

ACKNOWLEDGMENTS

Authors would like to express their gratitude to Prof. Carlo Poloni, founder and president of ESTECO, for providing modeFRONTIER software free of charge for this project. This work was partially funded by the US Air Force Office of Scientific Research under grant FA9550-12-1-0440 monitored by Dr. Ali Sayir. The views and conclusions contained herein are those of the authors and should not be interpreted as necessarily representing the official policies or endorsements, either expressed or implied, of the US Air Force Office of Scientific Research or the U.S. Government. The U.S. Government is authorized to reproduce and distribute reprints for government purposes notwithstanding any copyright notation thereon.

REFERENCES

1. R.W. Cahn (Edited), *The Coming of Materials Science*, Pergamon Materials Series, Science Direct, vol. 5, 3-571, 2001.
2. http://www.msm.cam.ac.uk/phasetrans/2003/nickel.html
3. T.M. Pollock and S. Tin, Nickel-based superalloys for advanced turbine engines: Chemistry, Microstructure, and Properties, *AIAA Journal of Propulsion and Power*, 22, 361-374, 2006.
4. W.D. Callister and D.G. Rethwisch, *Materials Science and Engineering: An Introduction, 8th Edition.* John Wiley & Sons, 2010.
5. http://www.cmse.ed.ac.uk/AdvMat45/SuperEng.pdf
6. H.K.D.H. Bhadeshia, Neural networks in materials science, *ISIJ International*, 39, 966-979, 1999.
7. H.K.D.H. Bhadeshia and T. Sourmail, Design of creep-resistant steels: Success & failure of models, *Japan Soc. for the Promotion of Science*, *Committee on Heat-Resisting Materials and Alloys*, 44, 299-314, 200.

8. I.N. Egorov, Indirect optimization method on the basis of self-organization, *Proceedings of Optimization Techniques and Applications (ICOTA'98),* Curtin University of Technology, Perth, Australia, 2 (1998), 683-691.
9. C.A. Coello Coello, D.A. Van Veldhuizen and G.B. Lamont, *Evolutionary Algorithms for Solving Multi-Objective Problems,* Kluwer Academic Publishers, New York, 2002.
10. K. Deb, *Multi-Objective Optimization Using Evolutionary Algorithms*, John Wiley & Sons, 2002.
11. G.S. Dulikravich, I.N. Egorov, V.K. Sikka and G. Muralidharan, Semi-stochastic optimization of chemical composition of high-temperature austenitic steels for desired mechanical properties. 2003 TMS Annual Meeting, *Yazawa International Symposium: Processing and Technologies,* eds: F. Kongoli, K. Itakagi, C. Yamaguchi, and H.-Y. Sohn, (TMS Publication, San Diego, CA, March 2-6, 2003) (1), 801-814, 2003.
12. I.N. Yegorov-Egorov and G.S. Dulikravich, Optimization of alloy chemistry for maximum stress and time-to-rupture at high temperature. *10th AIAA/ISSMO Multidisciplinary Analysis and Optimization Conference*; paper AIAA-2004-4348, eds: A. Messac and J. Renaud, AIAA, Albany, NY, Aug. 30 – Sept. 1, 2004.
13. I.N. Egorov-Yegorov and G.S. Dulikravich, Chemical composition design of superalloys for maximum stress, temperature and time-to-rupture using self-adapting response surface optimization. *Materials and Manufacturing Processes*, 20 (3) 569-590, 2005.
14. G.S. Dulikravich and I.N. Egorov-Yegorov, Robust optimization of concentrations of alloying elements in steel for maximum temperature, strength, time-to-rupture and minimum cost and weight. *ECCOMAS – Computational Methods for Coupled Problems in Science and Engineering*; eds: Papadrakakis, E. Onate and B. Schrefler, Fira, Santorini Island, Greece, May 25-28, 2005.
15. G.S. Dulikravich and I.N. Egorov-Yegorov, Design of alloy's concentrations for optimized strength, temperature, time-to-rupture, cost and weight. *Sixth International Special Emphasis Symposium on Superalloys 718, 625, 706 and Derivatives*, ed: E.A. Loria, TMS Publications, Pittsburgh, PA, October 2-5, 2005, 419-428, 2005.
16. G.S. Dulikravich and I.N. Egorov, Optimizing chemistry of bulk metallic glasses for improved thermal stability, Symposium on Bulk Metallic Glasses, TMS 2006 Annual Meeting & Exhibition, eds: Liaw, P. K. and Buchanan, R. A., San Antonio, TX, March 12-16, 2006.
17. G.S. Dulikravich, I.N. Egorov, and N. Jelisavcic, Evolutionary optimization of chemistry of bulk metallic glasses, III European Conference on Computational Solid and Structural Mechanics, eds: Onate, E., Mota Soares, C. A., Papadrakakis, M., Schrefler, B. and Teixeira de Freitas, J., Lisbon, Portugal, June 5-8, 2006.
18. G.S. Dulikravich, A. Kumar, and I.N. Egorov, Titanium Based Alloy Chemistry Optimization for Maximum Strength, Minimum Weight and Minimum Cost Using JMatPro and IOSO Software, TMS Annual Meeting, Materials Informatics: Enabling Integration of Modeling and Experiments in Materials Science, ed: Rajan, K., New Orleans, LA, March 9-13, 2008.
19. G.S. Dulikravich, I.N. Egorov, and M.J. Colaco, Optimizing chemistry of bulk metallic glasses for improved thermal stability, *Modelling and Simulation in Materials Science and Engineering*, 16, 2008, 075010 (19pp).
20. S. Bhargava, G.S. Dulikravich, G. Murty, A. Agarwal and M.J. Colaco. Stress corrosion cracking resistant aluminum alloys: Optimizing concentrations of alloying elements and tempering, *Materials and Manufacturing Processes*, vol. 26, 2011, pp. 363-374.
21. G.S. Dulikravich and I.N. Egorov. Inverse Design of Alloys' Chemistry for Specified Thermo-Mechanical Properties by Using Multi-Objective Optimization, Chap. 8 in Computational Methods for Applied Inverse Problems (eds: Wang, Y. F., Yagola, A. G. and Yang, C. C.), Inverse and Ill-Posed Problems Series 56, Walter De Gruyter and Higher Education Press, P.R. China, ISBN: 978-3-11-025905-6, September 2012.
22. N. Chakraborti, Genetic algorithms in materials design and processing, *International Materials Reviews*, 49 (3-4), 246-260, 2004.
23. M.J. Colaço, G.S. Dulikravich and D. Sahoo, A response surface method-based hybrid optimizer, *Inverse Problems in Science and Engineering*, 16:6, 717 – 741, 2008.
24. M.J. Colaço, W.B. Silva, A.C. Magalhães and G.S. Dulikravich, Response surface methods applied to scarce and small sets of training points – a comparative study, EngOpt 2008 - International Conference on Engineering Optimization, Rio de Janeiro, Brazil, June 1-6, 2008.
25. M.J. Colaço and G.S. Dulikravich, A hybrid RBF based method for highly multidimensional response surfaces using scarce data sets, AIAA-2008-5892, 12th AIAA/ISSMO Multidisciplinary Analysis and Optimization Conference, Victoria, British Columbia, Canada, September 10-12, 2008.
26. R.J. Moral and G.S. Dulikravich, A hybridized self-organizing response surface methodology, AIAA-2008-5891, 12th AIAA/ISSMO Multidisciplinary Analysis and Optimization Conference, Victoria, British Columbia, Canada, September 10-12, 2008.
27. G.S. Dulikravich and M.J. Colaco, Hybrid optimization algorithms and hybrid response surfaces, *Plenary Lecture*, Eurogen2013, Las Palmas de Gran Canaria, Spain, October 7-9, 2013(to appear in Springer series 2014).
28. B.K. Giri, J. Hakanen, K. Miettinen and N. Chakraborti, Genetic programming through bi-objective genetic algorithms with study of a simulated moving bed process involving multiple objectives, *Applied. Soft. Comput.,* 13, 2613-2623, 2013.
29. R. Jha, F. Pettersson, G.S. Dulikravich, H. Saxen and N. Chakraborti, Evolutionary design of nickel based superalloys using data-driven genetic algorithms and related strategies, to appear in *Modelling and Simulation in Materials Science and Engineering*, 2014.

30. R. Jha, P.K. Sen and N. Chakraborti, Multi-objective genetic algorithms and genetic programming models for minimizing input carbon rates in a blast furnace compared with a conventional analytic approach, *Steel. Res. Int.,* 84, 2013, DOI: 10.1002/srin.201300074.
31. B.K. Giri, F. Pettersson, N. Chakraborti and H. Saxén, Genetic programming evolved through bi-objective genetic algorithms applied to a blast furnace, *Mater. Manuf. Process*., 28, 776-782, 2013.
32. A. Kumar, D. Chakrabarti and N. Chakraborti, Data-driven Pareto optimization for microalloyed steels using genetic algorithms, *Steel Res. Int.* 83, 169-174, 2012
33. Y. Ikeda, A new method of alloy design using a genetic algorithm and molecular dynamics simulation and its application to nickel-based superalloys, *Mater. T. JIM.,* 38, 771-779, 1997.
34. B. Bhattacharya, G.R.D. Kumar, A. Agarwal, S. Erkoç, A. Singh, N. Chakraborti, Analyzing Fe–Zn system using molecular dynamics, evolutionary neural nets and multi-objective genetic algorithms, *Comp. Mater. Sci.,* 46, 821-827, 2009
35. F. Tancret, Computational thermodynamics and genetic algorithms to design affordable γ'-strengthened nickel–iron based superalloys, *Modelling Simul. Mater. Sci. Eng.,* 20, Article No. 045012 (6pp), DOI: 10.1088/0965-0393/20/4/045012, 2012.
36. F. Pettersson, N. Chakraborti and H. Saxén, A genetic algorithms based multi-objective neural net applied to noisy blast furnace data, *Appl. Soft. Comput.*, 7, 387–397, 2007.
37. D.N. Mondal, K. Sarangi, F. Pettersson, P.K. Sen, H. Saxén and N. Chakraborti, Cu-Zn separation by supported liquid membrane analyzed through multi-objective genetic algorithms, *Hydrometallurgy,* 107, 112-123, 2011.
38. F. Pettersson, N. Chakraborti and S.B. Singh, Neural networks analysis of steel plate processing augmented by multi-objective genetic algorithms, *Steel. Res. Int.,* 78, 890-898, 2007.
39. P. Rajak, U. Tewary, S. Das, B. Bhattacharya, N. Chakraborti, Phases in Zn-coated Fe analyzed through an evolutionary meta-model and multi-objective Genetic Algorithms, *Comp. Mater. Sci.,* 50, 2502-2516, 2011.
40. H. Saxén and F. Pettersson, Method for selection of inputs and structure of feedforward neural networks, *Comput. Chem. Eng.* 30, 1038-1045, 2006.
41. http://en.wikipedia.org/wiki/IOSO
42. http://www.esteco.com/home/mode_frontier.html.
43. http://www.factsage.com/
44. I.M. Sobol, Uniformly distributed sequences with an additional uniform property, *USSR Computational Mathematics and Mathematical Physics*, (16) 236-242, 1976.
45. http://en.wikipedia.org/wiki/Feature_scaling
46. P. Mazzatorta and E. Benfenati, The importance of scaling in data mining for toxicity prediction, *J. Chem. Inf. Comput. Sci.,* 42, 1250-1255, 2002.
47. P.T. Boggs and J.W. Tolle, Sequential quadratic programming. *Acta Numerica*, 4, 1-51, 1995. doi:10.1017/S0962492900002518.
48. B.D. Cullity and C.D. Graham, *Introduction to Magnetic Materials, 2nd ed*., New York: Wiley-IEEE Press, 2008.
49. M.J. Colaço, G.S. Dulikravich and T.J. Martin, H.R.B. Orlande, Hybrid optimization with automatic switching among optimization algorithms, evolutionary algorithms and intelligent tools in engineering optimization, W. Annicchiarico, J. Périaux, M. Cerrolaza and G. Winter (Eds.), CIMNE, Barcelona, Spain 2004
50. M.J. Colaço, G.S. Dulikravich and T.J. Martin, Optimization of wall electrodes for electro-hydrodynamic control of natural convection effects during solidification, ASME paper IMECE2003-41703, ASME IMECE 2003, Washington, DC, November 16-21, 2003.
51. M.J. Colaço, G.S. Dulikravich and T.J. Martin, Optimization of wall electrodes for electro-hydrodynamic control of natural convection effects during solidification, *Materials and Manufacturing Processes*, vol. 19, issue 4, 719-736, 2004.
52. M.J. Colaço, G.S. Dulikravich and T.J. Martin, Reducing convection effects in solidification by applying magnetic fields having optimized intensity distribution (Keynote Lecture), In: ASME Summer Heat Transfer Conference, July, 2003.
53. G.S. Dulikravich, M.J. Colaço, T.J. Martin and S.Lee, Magnetized fiber orientation and concentration control in solidifying composites, in: Symposium on Materials Processing Under the Influence of Electrical and Magnetical Fields, TMS Annual Meeting, San Diego, CA, 2003.
54. G.S. Dulikravich, M.J. Colaço, T.J. Martin and S. Lee, An inverse method allowing user-specified layout of magnetized micro-fibers in solidifying composites, *Journal of Composite Materials*, vol. 37, no. 15, 1351-1365, 2003.
55. G.S. Dulikravich, M.J. Colaço, B.H. Dennis, T.J. Martin and S. Lee, Optimization of intensities and orientations of magnets controlling melt flow during solidification, *Materials and Manufacturing Processes*, vol. 19, no. 4, 695-718, 2004.
56. M.J. Colaço, H.R.B. Orlande, G.S. Dulikravich and F.A. Rodrigues, A comparison of two solution techniques for the inverse problem of simultaneously estimating the spatial variations of diffusion, ASME HTD, Volume 374, Issue 1, 221-230, 2003.

ANNEX A

Table 1: Upper and lower bounds of the major alloying elements in Ni base superalloy design [15]

	Min	Max
C (wt %)	0.13	0.20
Cr (wt %)	8.0	9.5
Co (wt %)	9.0	10.5
W (wt %)	9.5	11.0
Mo (wt %)	1.2	2.4
Al (wt %)	5.1	6.0
Ti (wt %)	2.0	2.9
Stress to rupture (N/mm^2)	907	1037
Time to rupture (Hours)	25.17	92.38

Table 2: Correlation values of linear fit of the metamodel prediction using modeFrontier [42]

	Stress to rupture	Time to rupture
AKR	0.9043	0.96
SVD	1	1
GP	1	1
KR	0.9944	0.9944
RBF	1	1
ED	0.4337	0.5965

Table 5: Phase distribution at 975 ºC calculated using FactSage [43]

	AKR	ED	GP	KR	RBF	SVD
Phase						
FCC	gram	gram	gram	gram	gram	gram
Co:Va	9.90E+00	9.71E+00	9.71E+00	9.66E+00	9.55E+00	1.02E+01
Cr:Va	8.73E+00	8.72E+00	9.03E+00	8.81E+00	9.10E+00	8.43E+00
Ni:Va	1.44E+01	1.45E+01	1.39E+01	1.61E+01	1.59E+01	1.23E+01
TOTAL :	3.30E+01	3.29E+01	3.27E+01	3.46E+01	3.45E+01	3.10E+01
Ni3Al(s)	4.32E+01	4.38E+01	4.25E+01	3.98E+01	3.98E+01	4.46E+01
Ni3Ti(s)	1.08E+01	1.09E+01	1.22E+01	1.22E+01	1.20E+01	1.18E+01
W(s)	1.02E+01	9.69E+00	9.90E+00	1.03E+01	1.07E+01	9.69E+00
Nb8C7(s)	1.22E+00	1.22E+00	1.22E+00	1.25E+00	1.22E+00	7.13E-01
Nb4C3(s)						5.04E-01
Mo(s)	8.76E-01	8.10E-01	8.54E-01	1.22E+00	9.55E-01	7.77E-01
Mo2B(s)	4.69E-01	4.69E-01	4.69E-01	4.69E-01	4.69E-01	4.69E-01
TiC(s)	2.55E-01	1.65E-01	1.15E-01	1.47E-01	1.51E-01	3.69E-01
ZrC4(s)	6.11E-02	6.11E-02	6.11E-02	6.11E-02	6.11E-02	6.11E-02
Ce_gamm	1.50E-02	1.50E-02	1.50E-02	1.50E-02	1.50E-02	1.50E-02
Y-a(s)	1.00E-02	1.00E-02	1.00E-02	1.00E-02	1.00E-02	1.00E-02

Table 3: Dimensionless Pareto candidates selected for thermodynamic calculations from various modules in modeFRONTIER [42]

	SVD	AKR	KR	GP	ED	RBF
Al	0.9898	0.7849	0.2793	0.6813	0.0176	0.8763
C	0.9996	0.7453	0.3815	0.2748	0.3255	0.4448
Co	0.9999	0.6563	0.4055	0.4609	0.8609	0.4560
Cr	0.0001	0.2876	0.3723	0.5821	0.2263	0.2791
Mo	0.0006	0.1777	0.8498	0.1394	0.0952	0.0596
Ti	0.8490	0.1892	0.6409	0.5777	0.1164	0.0861
W	0.0004	0.3851	0.4669	0.1667	0.5046	9.E-07
Stress	0.7095	0.7274	1.0220	0.8407	0.8640	1.0998
Time	0.6461	0.9196	0.7165	0.9511	1.0456	0.9591

Table 4: Phase distribution at 25 ºC calculated using FactSage [43]

	AKR	ED	GP	KR	RBF	SVD
PHASE						
BCC	gram	gram	gram	gram	gram	gram
Co:Va	2.82E-05	2.95E-05	3.44E-05	2.95E-05	3.32E-05	2.56E-05
Cr:Va	3.48E+00	3.65E+00	4.26E+00	3.65E+00	4.11E+00	3.16E+00
Ni:Va	8.19E-10	8.58E-10	1.00E-09	8.59E-10	9.65E-10	7.44E-10
TOTAL :	3.48E+00	3.65E+00	4.26E+00	3.65E+00	4.11E+00	3.16E+00
FCC	gram	gram	gram	gram	gram	gram
Co:Va	8.81E-02	9.36E-02	8.89E-02	9.99E-02	9.26E-02	7.84E-02
Cr:Va	2.20E+00	2.34E+00	2.22E+00	2.50E+00	2.31E+00	1.96E+00
Ni:Va	1.18E+01	1.25E+01	1.19E+01	1.34E+01	1.24E+01	1.05E+01
TOTAL :	1.41E+01	1.50E+01	1.42E+01	1.60E+01	1.48E+01	1.25E+01
Ni3Al(s)	4.32E+01	4.38E+01	4.25E+01	3.98E+01	3.98E+01	4.46E+01
Co3W(s)	1.72E+01	1.68E+01	1.68E+01	1.66E+01	1.64E+01	1.79E+01
Ni3Ti(s)	1.17E+01	1.15E+01	1.26E+01	1.27E+01	1.26E+01	1.32E+01
Cr4C(s)	3.22E+00	2.89E+00	3.06E+00	4.06E+00	5.38E+00	3.50E+00
Ni4W(s)	3.22E+00	2.61E+00	2.70E+00	2.82E+00	2.84E+00	2.50E+00
NbCo2(s)	2.50E+00	2.50E+00	2.50E+00	2.50E+00	2.50E+00	1.31E+00
Mo(s)	8.76E-01	8.10E-01	8.54E-01	1.25E+00	9.55E-01	7.77E-01
Mo2B(s)	4.69E-01	4.69E-01	4.69E-01	4.69E-01	4.69E-01	4.69E-01
ZrC4(s)	6.11E-02	6.11E-02	6.11E-02	6.11E-02	6.11E-02	6.11E-02
Ce_beta(s)	1.50E-02	1.50E-02	1.50E-02	1.50E-02	1.50E-02	1.50E-02
Y-a(s)	1.00E-02	1.00E-02	1.00E-02	1.00E-02	1.00E-02	1.00E-02